

## All-aqueous multiphase microfluidics

Yang Song,<sup>1,2</sup> Alban Sauret,<sup>3</sup> and Ho Cheung Shum<sup>1,2,a)</sup>

<sup>1</sup>*Department of Mechanical Engineering, the University of Hong Kong, Hong Kong*

<sup>2</sup>*HKU-Shenzhen Institute of Research and Innovation (HKU-SIRI), Shenzhen, Guangdong, China*

<sup>3</sup>*Department of Mechanical and Aerospace Engineering, Princeton University, Princeton, New Jersey 08544, USA*

(Received 1 September 2013; accepted 18 October 2013; published online 27 December 2013)

Immiscible aqueous phases, formed by dissolving incompatible solutes in water, have been used in green chemical synthesis, molecular extraction and mimicking of cellular cytoplasm. Recently, a microfluidic approach has been introduced to generate all-aqueous emulsions and jets based on these immiscible aqueous phases; due to their biocompatibility, these all-aqueous structures have shown great promises as templates for fabricating biomaterials. The physico-chemical nature of interfaces between two immiscible aqueous phases leads to unique interfacial properties, such as an ultra-low interfacial tension. Strategies to manipulate components and direct their assembly at these interfaces needs to be explored. In this paper, we review progress on the topic over the past few years, with a focus on the fabrication and stabilization of all-aqueous structures in a multiphase microfluidic platform. We also discuss future efforts needed from the perspectives of fluidic physics, materials engineering, and biology for fulfilling potential applications ranging from materials fabrication to biomedical engineering. © 2013 AIP Publishing LLC. [<http://dx.doi.org/10.1063/1.4827916>]

### I. INTRODUCTION

Aqueous two-phase systems (ATPSs) are formed by dissolving two incompatible solutes in water above the critical concentrations for phase separation.<sup>1</sup> Typical pairs of incompatible solutes are summarized in Table I. These incompatible solutes can redistribute in water and form immiscible aqueous phases, if the reduction in enthalpy is sufficient to overcome the energy cost associated with the increased entropy.<sup>2</sup> This often requires each solute species of an ATPS to interact more strongly with itself than with the other species, leading to the segregation of solute of the same species and phase separation. However, the segregation is incomplete and each phase usually still contains a small amount of molecules of the other species. For example, in the equilibrium phase diagram of PEG/dextran/H<sub>2</sub>O system, the dextran-rich phase contains a minute amount of PEG; similarly, the PEG-rich phase also contains dextran.<sup>3</sup> Compositions of equilibrium phases vary with the molecular weight of incompatible solutes, temperature and other salt additives. The incomplete separation leads to lower mixing entropy than a complete separation and thus reduces the energetic cost of phase separation.

Immiscible phases formed by the phase separation of ATPSs are free of organic solvents; thus they are biocompatible and eco-friendly in biomedical research studies and applications.<sup>4-7</sup> In the synthesis of biomaterials, such as protein microspheres and hydrogel beads, organic solvents are usually involved. Upon solidifying the dispersed phase to form solid materials, organic solvents must be extracted by repeated washing.<sup>8</sup> These tedious steps to remove the organic phases can be avoided when ATPSs are used to form emulsions. Moreover, when protein solutions are exposed to the oil phases, denaturation of proteins often occurs at the water-oil (w/o) interface, reducing

---

<sup>a)</sup>Electronic mail: [ashum@hku.hk](mailto:ashum@hku.hk). Telephone: +852 61597387.

TABLE I. List of common aqueous two-phase systems formed with biocompatible additives. In each column, solute A and solute B represent a pair of incompatible solutes. In addition, some proteins and polysaccharides, such as sodium caseinate and sodium alginate can also form a biocompatible ATPS.<sup>10</sup>

Solute A	Polyethylene glycol (PEG)	Dextran	Methylcellulose
Solute B	Dextran	PEG	Dextran
	Polyvinyl alcohol (PVA)	PVA	PVA
	Polyvinyl pyrrolidone (PVP)	PVP	PVP
	Tripotassium phosphate (K <sub>3</sub> PO <sub>4</sub> )	Methylcellulose	Na <sub>2</sub> HPO <sub>4</sub>
	Sodium citrate or Sodium sulfate		

the bioactivity of the proteins.<sup>9</sup> The use of ATPS can significantly alleviate the concerns on the detrimental effects of organic solvents to the bioactivity of proteins and the viability of cells.<sup>10</sup>

With traditional methods for fabricating all-aqueous emulsions, such as vortex mixing<sup>11</sup> and homogenization,<sup>12</sup> the sizes and structures of the resultant all-aqueous emulsions can hardly be controlled. With recent progress in microfluidic technology, immiscible aqueous phases are precisely manipulated in microchannels, allowing the fabrication of all-aqueous emulsions and jets with excellent control. The approach of all-aqueous multiphase microfluidics will facilitate many biomedical studies that use ATPS as the medium, such as efficient molecular or cellular extraction,<sup>13,14</sup> and biomaterials synthesis.<sup>11,15</sup> In the following sections, we will separately discuss two basic fluidic structures formed by ATPS using microfluidic techniques: jets and drops.

## II. MICROFLUIDIC MANIPULATION ON THE ALL-AQUEOUS JETS

Manipulation of all-aqueous jets in microfluidic devices has been shown to be a critical tool in the separation of DNA,<sup>16,17</sup> proteins,<sup>18,19</sup> and cells.<sup>20</sup> In comparison to water/oil systems, common ATPSs have much lower interfacial tension values, ranging from less than  $10^{-2}$  mN/m to 1 mN/m (Table II).<sup>21–25</sup> Upon contact between two immiscible aqueous phases in co-flowing microchannels, the growth rate of interfacial instability in an all-aqueous jet depends on the value of interfacial tension relative to the inertial and viscous forces. For two aqueous phases with a sufficiently large interfacial tension, typically more than 0.1 mN/m, the capillary force cannot be neglected; this often leads to the break-up of the jet<sup>26</sup> through Rayleigh-Plateau instability.<sup>27</sup> On the contrary, for ATPSs with interfacial tension lower than 0.1 mN/m, the capillary force can normally be neglected, when compared to viscous or inertia effects at typical flow rates larger than 10  $\mu$ l/h. Consequently, the two phases are usually separated by a long and straight interface. This water/water interface is sensitive to the vibrations<sup>28,29</sup> in the surrounding environment as long as the viscosities are not exceedingly large. To take advantage of this property, mechanical perturbations have been introduced to oscillate the jet phase, inducing breakup of the jet,<sup>28,29</sup> as shown in Figures 1(a)–1(c).

TABLE II. List of the maximum interfacial tension values of different aqueous two-phase systems documented in literature. Interfacial tension between two immiscible aqueous phases increases with the concentration of incompatible solutes of ATPSs. The PEG/salt system typically has a relatively large interfacial tension ( $10^{-1}$ –1 mN/m) and low viscosities (<20 mPa·s); while the protein/polysaccharide system typically has an ultra-low interfacial tension ( $\leq 10^{-2}$  mN/m) and a relatively high viscosity (>50 mPa·s).

PEG/salt system <sup>21</sup>	PEG/Na <sub>2</sub> CO <sub>3</sub> 1.99 mN/m	PEG/K <sub>2</sub> HPO <sub>4</sub> 1.19 mN/m	PEG/Na <sub>2</sub> SO <sub>4</sub> 0.80 mN/m
PEG/polysaccharide system	PEG/dextran <sup>22</sup> 0.35 mN/m		PEG/maltodextran <sup>23</sup> 0.12 mN/m
Protein/polysaccharide system	gelatin/dextran <sup>24</sup> 0.03 mN/m		Sodium caseinate/Sodium alginate <sup>25</sup> 0.02 mN/m

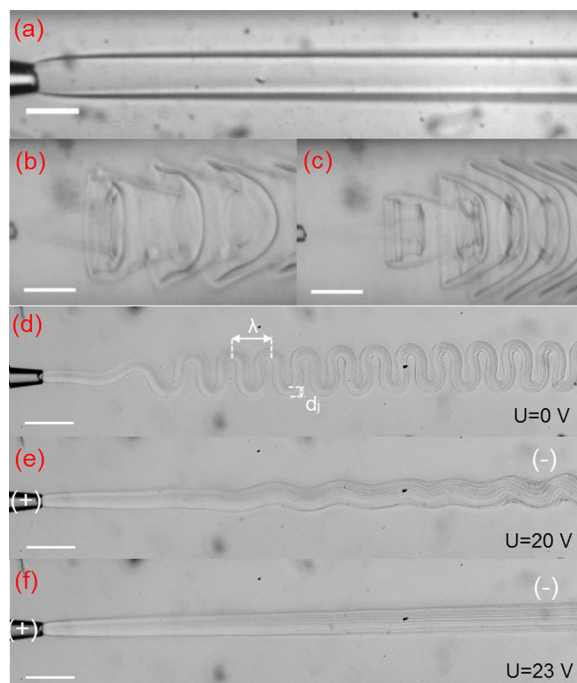


FIG. 1. Microscopic images of w/w jets with induced structures in microfluidic channels. A straight w/w jet is perturbed by hydrodynamic vibration at the frequency of (a) 0 Hz, (b) 7 Hz and (c) 10 Hz. Reprinted with permission from Sauret *et al.*, *Lab Chip* **12**, 3380, (2012). Copyright 2012 The Royal Society of Chemistry. A folded viscous w/w jet is manipulated by electrical charging at applied DC voltages of (d) 0 V, (e) 20 V, and (f) 23 V. The positions of the cathode and the anode are illustrated by the symbols (+) and (-) in (f), respectively. Scale bar is 200  $\mu\text{m}$ . Reprinted with permission from Song *et al.*, *Chem. Commun.* **49**, 1726 (2013). Copyright 2013 the Royal Society of Chemistry.

Other phenomena may also arise as the properties of the fluids change. For example, the viscosity of a jet increases drastically with the concentration of the dissolved polyelectrolytes. For sufficiently large viscosity ( $\eta$ ) ratio between the inner jet and outer continuous phase, typically  $\eta_{\text{in}}/\eta_{\text{out}} > 15$ , the w/w jet folds periodically to minimize the dissipation,<sup>30,31</sup> as illustrated in Figure 1(d). Such folding enhances the convective mixing in the microchannels<sup>32</sup> and is thus potentially useful in the applications of chemical synthesis, where mixing of different components is preferred. However, in the separation of proteins or cells of different species, collection of different components from a twisted jet is more difficult than from a straight jet. To avoid the viscous folding, an electrical charging approach has been applied.<sup>31</sup> To deform a w/w jet by an electrical field, a polyelectrolyte, such as sodium dextran sulfate (SDS), is firstly dissolved in the dextran-rich aqueous phase. Upon charging the inner and outer phases by a direct current (DC) power supply, the dextran sulfate anions repel each other and maximize the intermolecular distance among them, leading to the expansion of the crowded polymer network dissolved in the jet phase. Because of the expansion, the fluid velocity in the jet decreases, and the viscous inner jet no longer folds to minimize the viscous dissipation. Therefore, the charged jet straightens when the applied voltage reaches a critical value, as shown in Figures 1(e) and 1(f). Upon removal of the charging, the jet starts to fold. These findings suggest that a viscous w/w jet with high concentrations of dissolved polyelectrolytes can be manipulated through electrical charging and discharging. The practicality and biocompatibility of this approach for separating biomolecules from viscous fluids needs to be further investigated.

### III. MICROFLUIDIC FABRICATION OF ALL-AQUEOUS EMULSION DROPLETS

While microfluidic devices enable the generation of water-in-oil (w/o) or oil-in-water (o/w) emulsions with high monodispersity and control over droplet shapes and structures,<sup>33</sup> formation of monodisperse w/w emulsion is not always achieved in typical microfluidic channels owing

to the low interfacial tension of such systems. While direct droplet formation is observed in the PEG/salt system<sup>26</sup> with relatively high interfacial tension, breakup of all-aqueous jets in the low interfacial tension systems is usually difficult and results in polydisperse droplets because of the large Capillary and Weber numbers.<sup>34</sup> To assist the breakup of a w/w jet into monodisperse drops, we discuss two recently developed methods to generate all-aqueous emulsion.

### A. Hydrodynamic perturbation induced droplet formation

To induce the breakup of a w/w jet, a vibration source is introduced in the system to generate initial corrugations on the surface of a w/w jet. These vibrations can be incorporated into the microfluidic devices by embedding a piezoelectric actuator in the channel wall<sup>29,35</sup> or by using a mechanical vibrator that squeezes the soft tubing connected to the incoming channel.<sup>28,36</sup> The vibrator imposes fluctuations to the driving pressure and modulates the instantaneous flow rate of the perturbed phase, changing locally the diameters of the w/w jet. The shape of the corrugated jet can be controlled by applying appropriate frequency and amplitude of perturbation, as shown in Figures 2(a) and 2(b). Following the Rayleigh-Plateau instability,<sup>27</sup> corrugations induced by perturbation grow and accelerate the jet breakup process when the applied frequency  $f_p$  is below a critical value, given by  $f_p^* = Q_{in}/(2\pi^2 r_{jet}^3)$ ,<sup>36,37</sup> where  $Q_{in}$  is the flow rate of the dispersed phase and  $r_{jet}$  is the radius of cylindrical jets. At an optimal frequency of perturbation, the growth rate of the Rayleigh-Plateau instability reaches a maximum value, corresponding to the fastest breakup of w/w jets.<sup>28</sup> Meanwhile, with an increasing intensity of perturbation, the initial amplitude of the corrugations on the jet surface also increases, as demonstrated by the data in Figure 2(c).<sup>38</sup> At sufficiently large perturbation amplitude and an appropriate band of frequency, the growth rate reaches a maximum value. Under the optimal condition, the w/w jet is most likely to break up at the tip of the injection nozzle. Emulsion droplets formed in this dripping regime achieve a high uniformity in size,<sup>37,38</sup> with a polydispersity of less than 3%.<sup>37</sup> The average diameter of the resulting droplets,  $D_{drop}$ , is related to the forcing frequency through the expression  $D_{drop} = (6Q_{in}/\pi f)^{1/3}$ .<sup>29</sup> When the frequency of perturbation exceeds the critical value,  $f_p^*$ , the growth rate of Rayleigh-Plateau's instability on a perturbed jet diminishes or even becomes null. Consequently, perturbation only induces corrugations, which do not grow in amplitude or break up into droplets.

The ability to manipulate emulsion structure provides versatility in satisfying the needs of the applications. All-aqueous emulsions with structures of higher complexity can be generated based on the perturbation approach. A w/w/w double emulsion can be prepared by oscillating a w/w/w compound jet<sup>29</sup> or applying multiple stages of emulsification.<sup>36</sup> The number and diameters of the innermost liquid cores are adjusted by varying the frequency of perturbation and flow rates. Double emulsion can also be obtained by utilizing phase transition in w/w single emulsion droplets. For instance, a single-phase droplet with dissolved PEG and dextran can be reversibly converted into double emulsion upon extracting water out of the droplet phase<sup>37,39</sup> or decreasing temperature to induce phase separation.<sup>40</sup>

So far, the perturbation approach has not been demonstrated in the all-aqueous system with dynamic viscosity of 100 mPa·s or above. An efficient breakup of a viscous w/w jet is restricted by the low growth rate of the Rayleigh-Plateau instability,<sup>38</sup> and the optimal frequency of perturbation needs to be reassessed, taking into account the viscoelastic properties of non-Newtonian fluid systems. Formation of monodisperse droplets from viscous fluids also needs to be addressed in further study.

### B. Electro-hydrodynamic forcing induced droplet formation

Electrostatic force can be an alternative trigger to break up a w/w jet in microfluidic channels. For example, an electrical chopping approach leads to splitting of droplets from a w/w jet, as demonstrated in Figure 3. This method typically requires two incompatible solutes with different electrophoretic mobility, such as tetrabutylammonium bromide (TBAB) and ammonium sulfate (AS).<sup>41</sup> Upon applying a DC electrical field, the ammonium sulfate solute with the higher mobility moves faster to the electrodes than the other solute, leading to fission of the

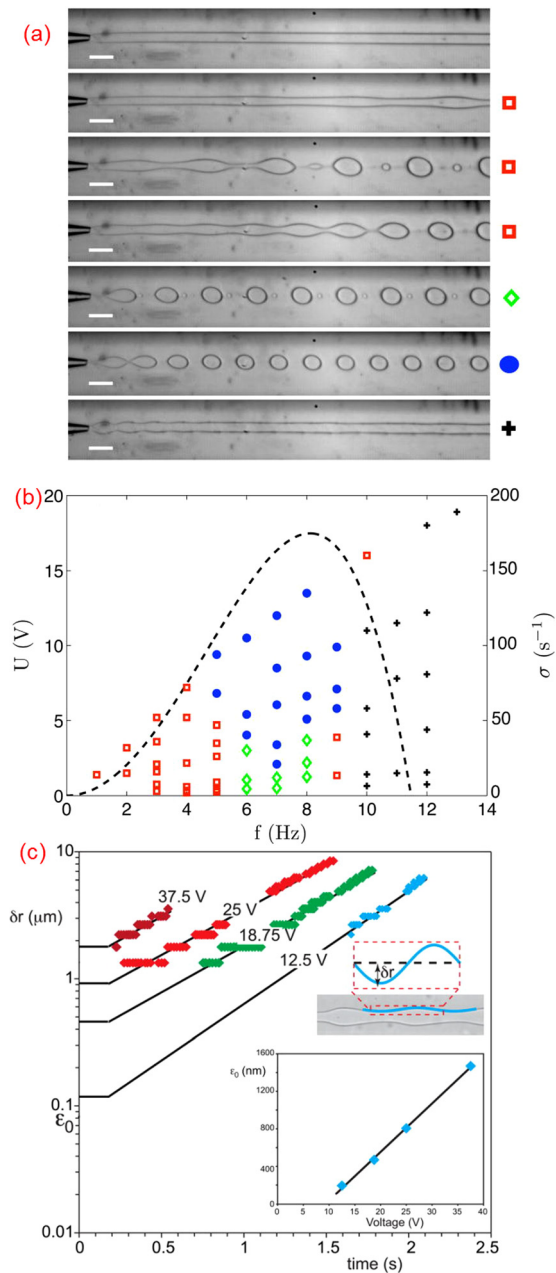


FIG. 2. Forced breakup of a w/w jet induced by hydrodynamic perturbation. (a) and (b) Breakup behaviors of a w/w jet triggered by forced oscillations at different perturbation frequency,  $f$ . Within an optimal range of frequency, monodisperse w/w droplets are generated, without satellite droplets, as shown by the blue dots. Scale bar is  $200 \mu m$ . Reprinted with permission from Sauret and Shum, *Appl. Phys. Lett.* **100**, 154106 (2012). Copyright 2012 American Institute of Physics. (c) Perturbation amplitude,  $\delta r$ , increases with the intensity of vibration, which is regulated by the DC voltages applied to a piezoelectric vibrator. Reprinted with permission from Geschiere *et al.*, *Biomicrofluidics* **6**, 022007 (2012). Copyright 2012 American Institute of Physics.

droplets from the AS-rich phase. Nevertheless, practical considerations, such as the polydispersity of droplet sizes, as well as the stability of proteins in the electrical field, still needs to be further explored before the approach can be fully applied to produce droplets. When incompatible solutes with similar electrophoretic mobility are charged in water, the relative motion of the emulsion phase is insufficient to result in droplet formation at low voltages. When higher voltages are exerted, the boundary of the two aqueous phases becomes blurry.<sup>42</sup> This phenomenon may be related to the increased electrostatic repulsion among charged solutes, which weakens

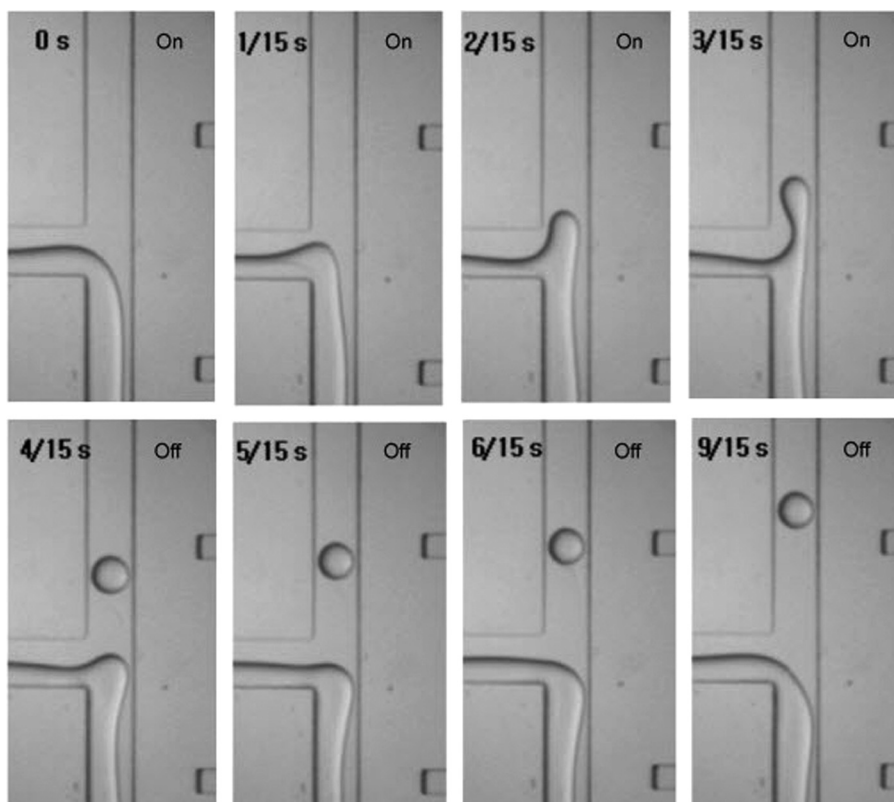


FIG. 3. Formation of a w/w emulsion induced by electro-hydrodynamic chopping. The width of channel is  $200\ \mu\text{m}$ . Reprinted with permission from Song *et al.*, *J. Chromatogr. A* **1162**, 180 (2007). Copyright 2007 Elsevier.

the interaction of solutes of the same species, thus elevating the energy cost of phase separation.

Inspired by the above approach, the emulsion and continuous aqueous phases are separated by a middle phase of air, preventing the mixing of charged solutes induced by high voltage. The resultant electrospray approach has traditionally been applied to single-phase aqueous solutions,<sup>43–46</sup> but it has not been applied to generate all-aqueous emulsions. With this approach, the dispersed phase of 8 wt. % PEG ( $M_w = 8000$ ) solution charged with a high DC voltage is sprayed into its immiscible aqueous phase of 15 wt. % dextran ( $M_w = 500\ 000$ ) solution through air. The large surface tension between the dispersed phase and air helps to break up the jet quickly into droplets, as illustrated schematically in Figure 4(a). By increasing the applied electrical field from  $2.1\ \text{kV/cm}$  to  $2.5\ \text{kV/cm}$ , the diameters of the produced droplets are significantly reduced from  $810\ \mu\text{m}$  to  $120\ \mu\text{m}$ , as shown in Figure S1 in the supplementary material.<sup>47</sup> A dripping-to-jetting transition is observed upon an increase in the applied voltage. In the dripping regime, the charged jet immediately breaks up at the end of the spraying nozzle, yielding monodisperse droplets with a polydispersity of less than 5%, as shown in Figure 4(b). In the jetting regime, polydisperse droplets are formed at the end of the Taylor cone. A reduction in the size of the spraying nozzle reduces the diameter of the jet, thus facilitating the fast formation of droplets in the electro-dripping regime.

The core-shell structured emulsion can also be generated with the all-aqueous electrospray approach. A round capillary with a tapered nozzle is coaxially inserted into another tapered squared capillary, forming a co-flowing geometry (Figure 4(a)). Two immiscible aqueous phases of 10% dextran ( $M_w = 500\ 000$ ) and 8 wt. % PEG ( $M_w = 8000$ ) solutions are separately injected into the inner and outer glass capillaries, forming a dextran-in-PEG jet. The PEG-rich phase is charged by a high-voltage power supply and the compound jet is forced to go through a ring-shaped counter electrode under electrostatic forces. Upon breakup of the jet, core-shell

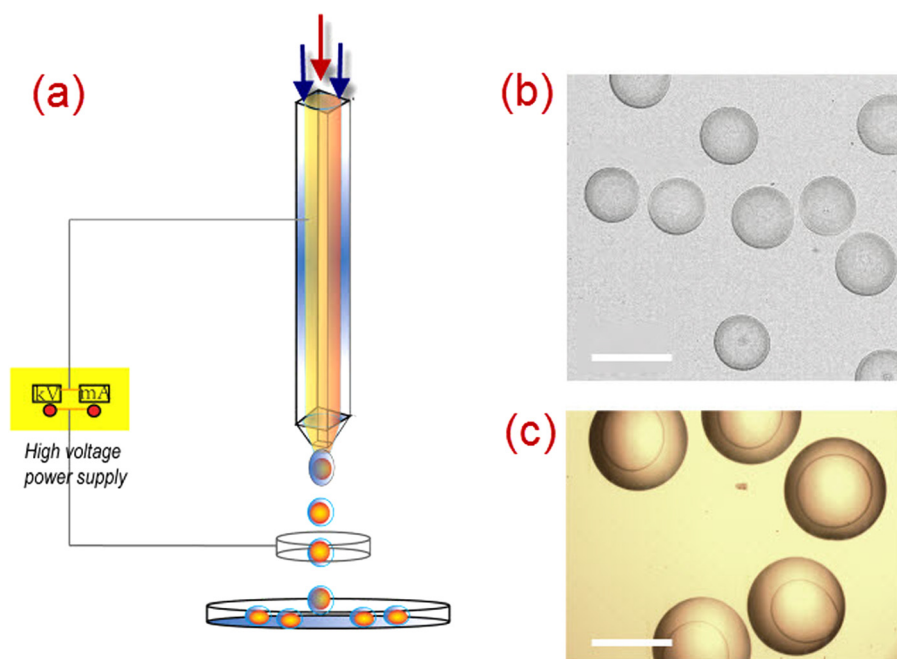


FIG. 4. (a) Schematic of the formation of aqueous droplets in the all-aqueous electrospay approach; (b) optical microscopic images of monodisperse aqueous droplets produced by all-aqueous electrospay; (c) microscopic images of all-aqueous emulsions with a core-shell structure; droplets are collected on a glass slide. Scale bar is  $200\ \mu\text{m}$ .

structured droplets finally fall into the continuous phase of a dextran solution or on the surface of a solid substrate (Figure 4(c)). The relative sizes of the core and shell of the emulsion can be easily adjusted by changing the flow rates ratios of the two fluids, as demonstrated in Figure s2<sup>47</sup> in the supplementary material. These findings suggest a potential way of fabricating all-aqueous emulsion using electrospay. Despite the high voltage involved, electrospay techniques have often been utilized for the encapsulation of cells in aqueous droplets;<sup>48</sup> therefore, biocompatibility of the all-aqueous electrospay approach is expected, though deserving further investigations.

We have summarized the current microfluidic techniques for producing all-aqueous emulsion droplets as well as their advantages and disadvantages in Table III.

#### IV. STABILIZATION OF THE ALL-AQUEOUS EMULSION

Although the all-aqueous emulsions with controlled and tunable structures have been generated with different approaches, all of these emulsions are only transiently stable and tend to

TABLE III. Comparison of different methods for producing all-aqueous emulsion droplets.

Methods	Advantages	Disadvantages
Hydrodynamic perturbation	Monodisperse droplets with tunable size Modifiable via post-processing of the droplets	Not applicable to ATPS with high viscosity or ultra-low interfacial tension;
Electro-hydrodynamic chopping	Modifiable via post-processing of the droplets	Not applicable for ATPS with similar electrophoretic mobility
All-aqueous electrospay	Applicable to viscous liquids Controllable sizes and structure Fast rate of droplets' generation.	Not amenable to post-processing of emulsion in microchannels

coalesce subsequently.<sup>15,36,37</sup> Stabilization of these emulsions is thus critical in both scientific studies and practical applications.

### A. All-aqueous emulsion templated materials

Stabilized emulsion structures can be produced by selectively solidifying the dispersed phases, forming hydrogel beads or capsules. To prevent the coalescence of droplets, photo-curable monomers such as PEGDA<sup>15</sup> or dextran-HEMA<sup>34</sup> have been added to the emulsion phase, and the fast photo-polymerization helps to solidify the emulsion within seconds. However, photo-polymerization typically generates toxic free radicals, potentially harming the encapsulated species, especially the living ones.<sup>49</sup> To achieve radical-free gelation, the emulsion phase can be solidified by diffusing harmless cross-linkers to the gel precursors in the emulsion phase.<sup>50</sup> For example, when the precursor of sodium alginate solution is used as the emulsion phase, the emulsion can be quickly solidified within a minute by introducing calcium ions.<sup>51</sup> Leakage of encapsulated species is negligible within the time scale of emulsion gelation. Nevertheless, many biocompatible gelation reactions, such as enzyme-induced gelation, last for hours to days,<sup>52</sup> where leakage of encapsulated species cannot be neglected. Therefore, a compact membrane must quickly form at the w/w interface, preventing the leakage of encapsulated species.

### B. Water/water interface-templated materials

Formation of a membrane at w/w interface remains as a new concept for stabilizing all-aqueous emulsion. The primary step involved is the aggregation of particles or macromolecular surfactants at the w/w interface. Submicron-sized latex microspheres and protein particles can be irreversibly trapped at the w/w interface. This feature indicates that the absorption energy is larger than the kinetic energy imposed by thermal activation.<sup>53</sup> With a sufficiently large concentration of protein particles and high w/w interfacial tension, protein particles successfully stabilize the PEG/dextran emulsion for a few weeks.<sup>54</sup> However, in the presence of a shear flow, these particles detach from the w/w interface and fail to stabilize the emulsion.<sup>53</sup> Strengthening the binding force among the protein particles may prevent the detachment from the interfaces induced by the shear flow, but this issue remains unexplored.

Self-assembly of macromolecules at the w/w interface provides another possible solution to stabilize the all-aqueous emulsions. To form stable emulsion, macromolecular surfactants should aggregate at the w/w interface and form a compact membrane. Aggregation of the surfactants at the w/w interface is strongly affected by their interactions with the dissolved solutes in aqueous phases. The presence of such interaction is confirmed by the observation of budding of liposomes encapsulating two immiscible aqueous phases,<sup>55,56</sup> as shown in Figure 5(a). In this example, two aqueous phases selectively approach the different lipid domains after extraction of water from the liposomes. The interaction between the membrane and the incompatible solutes also keeps the membrane at the w/w interface. This hypothesis is confirmed by using copolymers to form vesicles from the templates of w/w emulsions.<sup>57</sup> In this study, the copolymers of the PEG-polycaprolactone (PCL) and the dextran-PCL are separately added into the PEG-rich and dextran-rich phases. Upon vortex mixing of the two phases, the two copolymers spontaneously aggregate at the w/w interface, as shown in Figures 5(b) and 5(c). More importantly, the PCL moieties facilitate the formation of a compact membrane, probably due to the hydrophobic interactions. This inspiring work suggests that the assembly of asymmetric giant vesicles does not necessarily rely on the presence of organic solvents, and the w/w interface can be stabilized by macromolecular surfactants. This approach is expected to work also for the self-assembly through other types of intermolecular forces, such as electrostatic forces, covalent bonding, and van der Waals' forces.<sup>58</sup>

## V. CHALLENGES AND OPPORTUNITIES

While a series of advances in the all-aqueous multiphase microfluidics have been demonstrated, many challenges remain unaddressed.

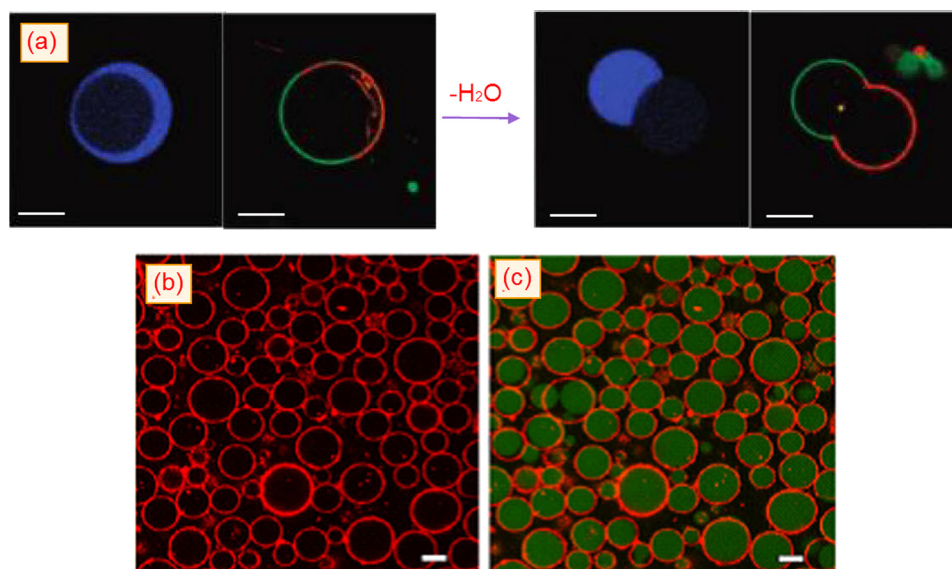


FIG. 5. Interfacial aggregation and assembly of macromolecules are affected by the local compositions of the aqueous phases. (a) Dextran-rich and PEG-rich phases selectively approach the different domains of a budding liposome upon extraction of water. Reprinted with permission from Cans *et al.*, *J. Am. Chem. Soc.* **130**, 7400 (2008). Copyright 2008 ACS Publications. (b) and (c) Conjunctions of the copolymers PEG-PCL and dextran-PCL aggregates at the interface of dextran-in-PEG emulsion, yielding asymmetrical vesicles. Scale bar is  $10\ \mu\text{m}$ . Reprinted with permission from Zhang *et al.*, *J. Controlled Release* **147**, 413 (2010). Copyright 2010 Elsevier.

### A. Design new ATPSs

Most of the ATPSs have ultra-low interfacial tension and relatively large dynamic viscosity; thus, formation of w/w emulsion cannot rely on spontaneous jet breakup in conventional microfluidic designs. Successful generation of w/w emulsion in modified device geometries is limited to ATPSs with interfacial tension higher than  $0.1\ \text{mN/m}$  and dynamic viscosity lower than  $10^2\ \text{mPa}\cdot\text{s}$ , such as the dextran/PEG system and the PEG/salt system. In ATPS containing a protein-rich phase or other polyelectrolyte phases, breakup of the w/w jet usually restricted by ultra-low interfacial tension and high viscosities of the ATPS, even using hydrodynamic perturbations. The appropriate range of conditions for controlled droplet generation with the hydrodynamic perturbation approach remains unexplored. New strategies to break up viscous all-aqueous jets are necessary for practical applications. The all-aqueous electrospay represents a promising approach in this area. The high voltage applied provides a strong pulling on the viscous jet and the large surface tension induces breakup of the jet. Alternatively, new ATPSs with interfacial tension higher than  $10^{-4}\ \text{N/m}$  and dynamic viscosity of less than  $10^2\ \text{mPa}\cdot\text{s}$  need to be investigated; this will increase the range of materials to meet the needs of the emerging applications using microfluidic technologies. Although such ATPSs have been found in systems composed of inorganic salts,<sup>21,59</sup> the concentrated salt solution phases are often too harsh an environment for proteins and cells, partly due to the inevitably high osmolarity.<sup>1</sup> Instead, ATPS composed of biocompatible macromolecules are promising alternatives that deserve further investigation. To discover ATPSs that meet the required standards of fluid properties for the target applications, the molecular structures of incompatible solutes need to be custom-designed, with special considerations on the intermolecular forces and their conformations at the w/w interface.

### B. New interfacial properties for fluid mechanics

From a physics of fluid point of view, the ATPS is a novel model system to study fluid behaviors unique to systems with a low interfacial tension and a thick interface. So far, the theoretical prediction on the breakup of w/w jet fails to match with the experimental observation.<sup>38</sup>

As opposed to the thin w/o interface, the incomplete phase separation in ATPS indicates a lower energy barrier for dissociation and migration of some molecules from their native phase to the other phase. In other words, the presence of local water flow may change the dynamic distribution of the incompatible solutes and the interfacial properties as well.<sup>60,61</sup> Therefore, the thickness of the w/w interface needs to be redefined and investigated, especially when non-equilibrium phases of ATPS are investigated.

In comparison to the w/o interface with large interfacial tension, creation of new w/w interfaces with the same surface area costs less energy. With the assistance of hydrodynamic or electrostatic perturbation, controlled breakup of the w/w jet can be induced at a low perturbation frequency, typically less than  $10^2$  Hz. So far, the w/w emulsions fabricated through microfluidic approaches have diameters ranging from few tens of micrometers to hundreds of micrometers, which are one to two orders of magnitude higher than the droplet size achieved in the water/oil system. To further reduce the dimension of the all-aqueous emulsion to submicron size range, new strategies of generating all-aqueous emulsion with a high frequency of more than  $10^4$  Hz are needed. This would eventually broaden the applications of all-aqueous emulsion, such as in gene delivery<sup>62</sup> and cellular imaging.<sup>63</sup>

### C. New approaches for materials fabrication

While the fabrication of multi-functional materials can be templated from emulsions with complex structures, the concept has not been sufficiently adapted to the all-aqueous systems. With water/oil multiple emulsions as templates, multiple polymersomes<sup>64</sup> and core-shell particles<sup>65</sup> are fabricated to program the release kinetics of drugs; Janus capsules formed from templates of compartmentalized double emulsion encapsulate and deliver different species without cross contamination.<sup>66</sup> By contrast, development of all-aqueous emulsion-templated materials is at its infancy. The challenges and opportunities involved require exploration to different material types at different size scales. In the sub-micron size range, self-assembly of macromolecules and particles in the ATPS is affected by their interaction with the surrounding molecules. A deeper understanding of these interactions potentially allow control over the conformation of biomolecules in all-aqueous multiphase systems, and guide the assembly of copolymers, macromolecules and colloids into desired aggregates. In the size range of micrometers or higher, generation of multiple all-aqueous emulsions with flexible structures and dimensions provides versatility needed in designing multi-functional materials, such as drug delivery vehicles, biosensors, microreactors and micro-containers. Stacking of emulsions and emulsion-templated materials in large scale will result in highly organized hierarchical structures, including micro-fibers,<sup>67</sup> membrane<sup>68</sup> and porous scaffolds.<sup>69</sup> Successful construction of these structures is a prerequisite towards functional replication in artificial materials, such as tissue-like scaffolds<sup>70</sup> and photonic materials.<sup>71</sup> Hierarchical assembly of materials can be guided by either all-aqueous phases or their interface. In the assembly of functional biomimetic units, droplet networks constructed through 3-D printing<sup>72</sup> and droplet-packing in chambers<sup>73</sup> bring new promises. Meanwhile, hierarchical assembly of nano-particles has been investigated at the interfaces of two miscible aqueous phases.<sup>74</sup> When this concept is applied to immiscible aqueous phases, assembly of nano-particles can be confined at the w/w interface without extension into bulk aqueous phases.

### D. All-aqueous multiphase medium as a model for biological organelles

Aqueous two-phase systems create an excellent all-aqueous environment for the mimicking of cytoplasmic environments in cells.<sup>75</sup> During the differentiation of a single-cell embryo, RNA-binding proteins are found to localize themselves by partitioning; thus, aqueous phase separation may have played an important role in the structuring and assembly of biological components.<sup>76</sup> Biomolecules selectively partition into different aqueous phases, and this selectivity can be enhanced in the presence of protein ligands or enzymes.<sup>77</sup> The partition of biomolecules in the ATPS increases their local concentrations; thus biochemical reactions and molecular assembly are accelerated.<sup>78</sup> Transfer of biomolecules among the different chambers

formed by aqueous phases could be regulated by a semi-permeable membrane, which allows a steady and dynamic microenvironment for cellular metabolism. Compartmentalization of different biomolecules and biological organelles in all-aqueous emulsion-templated vesicles represents a new route to achieve the cyto-mimetic compartments.<sup>75</sup> This provides opportunities to investigate the activities of biomolecules and biological organelles, as well as their synergetic interactions. Once the artificial cyto-mimetic compartments are developed, synthesis of proteins and DNA can be carried out in the physiological microenvironment, where the molecular structure and biological functions of these biomolecules are best preserved.

## VI. SUMMARY

In this paper, we have reviewed recent progress in the generation of all-aqueous emulsions and jets in microfluidic systems. Interestingly, microfluidic methods have been shown to be a potential tool for manipulating all-aqueous multiphase systems with variable sizes and structures. Despite recent advances in controlling the all-aqueous structure hydrodynamically, mechanically, and electrostatically, the complexity of the all-aqueous structures as well as their applications have not yet caught up with the state-of-art analogues of the water- and organic-solvent-based emulsions. In addition, diverse and robust strategies for stabilizing the all-aqueous emulsion remain lacking. Nevertheless, the all-aqueous multiphase structures, together with the emulsion-templated approach comprise a biocompatible platform for encapsulation of macromolecular species, synthesis of functional materials and mimicking of cellular microenvironments. Despite challenges in the areas of fluid mechanics and molecular assembly, the all-aqueous multiphase microfluidics is surely a promising research area that will lead to fundamental understanding of novel interfacial phenomena and biomaterials, as well as important applications in areas including biomedical engineering, food processing and cosmetics manufacture.

## ACKNOWLEDGMENTS

This research was supported by the Early Career Scheme (HKU 707712P) from the Research Grants Council of Hong Kong, the Young Scholar's Program (NSFC51206138/E0605) from the National Natural Science Foundation of China, the Basic Research Program-General Program (JC201105190878A) from the Science and Technology Innovation Commission of Shenzhen Municipality, as well as the Seed Funding Programme for Basic Research (201211159090) and Small Project Funding (201109176165) from the University of Hong Kong.

- <sup>1</sup>A. D. Diamond and J. T. Hsu, *Adv. Biochem. Eng./Biotechnol.* **47**, 89–135 (1992).
- <sup>2</sup>R. Hatti-Kaul, *Mol. Biotechnol.* **19**, 269–277 (2001).
- <sup>3</sup>A. D. Diamond and J. T. Hsu, *Biotechnol. Tech.* **3**, 119–124 (1989).
- <sup>4</sup>C. K. Su and B. H. Chiang, *Process Biochem.* **41**, 257–263 (2006).
- <sup>5</sup>R. S. King, H. W. Blanch, and J. M. Prausnitz, *AIChE J.* **34**, 1585–1594 (1988).
- <sup>6</sup>D. M. Brunette and J. E. Till, *J. Membr. Biol.* **5**, 215–224 (1971).
- <sup>7</sup>A. D. Diamond and J. T. Hsu, *AIChE J.* **36**, 1017–1024 (1990).
- <sup>8</sup>F. Y. Hsu, S. Chueh, and Y. J. Wang, *Biomaterials* **20**, 1931–1936 (1999).
- <sup>9</sup>M. van de Weert, J. Hoehstetter, W. E. Hennink, and D. J. A. Crommelin, *J. Control. Release* **68**, 351–359 (2000).
- <sup>10</sup>B. Sivasankar, *Bioseparations: Principles and Techniques* (Prentice-Hall of India Private Limited, New Delhi, 2006).
- <sup>11</sup>R. J. H. Stenekes, O. Franssen, E. M. G. van Bommel, D. J. A. Crommelin, and W. E. Hennink, *Int. J. Pharm.* **183**, 29–32 (1999).
- <sup>12</sup>Y. A. Antonov, P. V. Puyvelde, P. Moldenaers, and K. U. Leuven, *Biomacromolecules* **5**, 276–283 (2004).
- <sup>13</sup>S. Hardt and T. Hahn, *Lab Chip* **12**, 434–442 (2012).
- <sup>14</sup>K. Vijayakumar, S. Gulati, A. J. deMello, and J. B. Edel, *Chem. Sci.* **1**, 447–452 (2010).
- <sup>15</sup>H. C. Shum, J. Varnell, and D. A. Weitz, *Biomicrofluidics* **6**, 012808 (2012).
- <sup>16</sup>T. Hahn and S. Hardt, *Soft Matter* **7**, 6320–6327 (2011).
- <sup>17</sup>T. Hahn and S. Hardt, *Anal. Chem.* **83**, 5476–5479 (2011).
- <sup>18</sup>R. J. Meagher, Y. K. Light, and A. K. Singh, *Lab Chip* **8**, 527–532 (2008).
- <sup>19</sup>G. Münchow, S. Hardt, J. P. Kutter, and K. S. Drese, *Lab Chip* **7**, 98–102 (2007).
- <sup>20</sup>K. H. Nam, W. J. Chang, H. Hong, S. M. Lim, D. I. Kim, and Y. M. Koo, *Biomed. Microdevices* **7**, 189–195 (2005).
- <sup>21</sup>Y. Wu, Z. Zhu, and L. Mei, *J. Chem. Eng. Data* **41**, 1032–1035 (1996).
- <sup>22</sup>D. Forciniti, C. K. Hall, and M. R. Kula, *J. Biotechnol.* **16**, 279–296 (1990).
- <sup>23</sup>A. D. Giraldo-Zuniga, J. S. R. Coimbra, D. A. Arquete, L. A. Minim, L. H. M. Silva, and M. Cristina Maffia, *J. Chem. Eng. Data* **51**, 1144–1147 (2006).
- <sup>24</sup>P. Ding, B. Wolf, W. J. Frith, A. H. Clark, I. T. Norton, and A. W. Pacey, *J. Colloid Interface Sci.* **253**, 367–376 (2002).

- <sup>25</sup>M. Simeone, A. Alfani, and S. Guido, *Food Hydrocolloids* **18**, 463–470 (2004).
- <sup>26</sup>Y. Lu, Y. Xia, and G. Luo, *Microfluid Nanofluid* **10**, 1079–1086 (2011).
- <sup>27</sup>J. Eggers and E. Villermaux, *Rep. Prog. Phys.* **71**, 036601 (2008).
- <sup>28</sup>A. Sauret, C. Spandagos, and H. C. Shum, *Lab Chip* **12**, 3380–3386 (2012).
- <sup>29</sup>I. Ziemecka, V. V. Steijn, G. J. M. Koper, M. T. Kreutzer, and J. H. van Esch, *Soft Matter* **7**, 9878–9880 (2011).
- <sup>30</sup>T. Cubaud and T. G. Mason, *Soft Matter* **8**, 10573–10582 (2012).
- <sup>31</sup>Y. Song, Z. Liu, T. T. Kong, and H. C. Shum, *Chem. Commun.* **49**, 1726–1728 (2013).
- <sup>32</sup>T. Cubaud and T. G. Mason, *Phys. Rev. Lett.* **96**, 114501 (2006).
- <sup>33</sup>R. K. Shah, H. C. Shum, A. C. Rowat, D. Lee, J. J. Agresti, A. S. Utada, L. Y. Chu, J. W. Kim, A. Fernandez-Nieves, C. J. Martinez, and D. A. Weitz, *Mater. Today* **11**, 18–27 (2008).
- <sup>34</sup>I. Ziemecka, V. V. Steijn, G. J. M. Koper, and M. Rosso, *Lab Chip* **11**, 620–624 (2011).
- <sup>35</sup>A. Bransky, N. Korin, M. Khoury, and S. Levenberg, *Lab Chip* **9**, 516–520 (2009).
- <sup>36</sup>A. Sauret and H. C. Shum, *Appl. Phys. Lett.* **100**, 154106 (2012).
- <sup>37</sup>Y. Song and H. C. Shum, *Langmuir* **28**, 12054–12059 (2012).
- <sup>38</sup>S. D. Geschiere, I. Ziemecka, V. V. Steijn, G. J. M. Koper, J. H. van Esch, and M. T. Kreutzer, *Biomicrofluidics* **6**, 022007 (2012).
- <sup>39</sup>J. B. Boreyko, P. Mruetusatom, S. T. Retterer, and C. P. Collier, *Lab Chip* **13**, 1295–1301 (2013).
- <sup>40</sup>M. S. Long, C. D. Jones, M. R. Helfrich, L. K. Mangeney-Slavin, and C. D. Keating, *Proc. Natl. Acad. Sci.* **102**, 5920–5925 (2005).
- <sup>41</sup>Y. S. Song, Y. H. Choi, and D. H. Kim, *J. Chromatogr. A* **1162**, 180–186 (2007).
- <sup>42</sup>C. Y. Lee, C. L. Chang, Y. N. Wang, and L. M. Fu, *Int. J. Mol. Sci.* **12**, 3263–3287 (2011).
- <sup>43</sup>K. Tang and A. Gomez, *J. Aerosol Sci.* **25**, 1237–1249 (1994).
- <sup>44</sup>A. Jaworek, *J. Microencapsulation* **25**, 443–468 (2008).
- <sup>45</sup>W. Deng, J. M. Klemic, X. Li, M. A. Reed, and A. Gomez, *J. Aerosol Sci.* **37**, 696–714 (2006).
- <sup>46</sup>H. Chen, Y. Zhao, Y. Song, and L. Jiang, *J. Am. Chem. Soc.* **130**, 7800–7801 (2008).
- <sup>47</sup>See supplementary material at <http://dx.doi.org/10.1063/1.4827916> for the feasibility to produce droplets with tunable sizes and structures through the all-aqueous electrospray technique.
- <sup>48</sup>M. Ma, A. Chiu, G. Sahay, J. C. Doloff, N. Dholakia, R. Thakrar, J. Cochen, A. Vegas, D. Chen, K. M. Bratlie, T. Dang, R. L. York, J. Hollister-Lock, G. C. Weir, and D. G. Anderson, *Adv. Healthcare Mater.* **2**, 768 (2013).
- <sup>49</sup>T. Rossow, J. A. Heyman, A. J. Ehrlicher, A. Langhoff, D. A. Weitz, R. Haag, and S. Seiffert, *J. Am. Soc.* **134**, 4983–4989 (2012).
- <sup>50</sup>B. Z. Li, L. J. Wang, and D. Li, *Carbohydr. Polym.* **88**, 912–916 (2012).
- <sup>51</sup>W. H. Tan and S. Takeuchi, *Adv. Mater.* **19**, 2696–2701 (2007).
- <sup>52</sup>P. Chr. Lorenzen, *Food Res. Int.* **40**, 700–708 (2007).
- <sup>53</sup>G. Balakrishnan, T. Nicolai, L. Benyahia, and D. Durand, *Langmuir* **28**, 5921–5926 (2012).
- <sup>54</sup>B. T. Nguyen, T. Nicolai, and L. Benyahia, *Langmuir* **29**, 10658–10664 (2013).
- <sup>55</sup>A. S. Cans, M. Andes-Koback, and C. D. Keating, *J. Am. Chem. Soc.* **130**, 7400–7406 (2008).
- <sup>56</sup>M. Andes-Koback and C. D. Keating, *J. Am. Chem. Soc.* **133**, 9545–9555 (2011).
- <sup>57</sup>Y. Zhang, F. Wu, W. Yuan, and T. Jin, *J. Controlled Release* **147**, 413–419 (2010).
- <sup>58</sup>K. A. Simon, P. Sejwal, R. B. Gerecht, and Y. Y. Luk, *Langmuir* **23**, 1453–1458 (2006).
- <sup>59</sup>L. H. M. Silva, M. C. H. Silva, R. C. Sousa, J. P. Martins, G. D. Rodrigues, J. S. R. Coimbra, and L. A. Minim, *J. Chem. Eng. Data* **54**, 531–535 (2009).
- <sup>60</sup>J. A. Pojman, C. Whitmore, M. L. Turco Liveri, R. Lombardo, J. Marszalek, R. Parker, and B. Zoltowski, *Langmuir* **22**, 2569–2577 (2006).
- <sup>61</sup>B. Zoltowski, Y. Chekanov, M. Jonathan, J. A. Pojman, and V. Volpert, *Langmuir* **23**, 5522–5531 (2007).
- <sup>62</sup>J. W. Hong, J. H. Park, K. M. Huh, H. Chung, I. C. Kwon, and S. Y. Jeong, *J. Controlled Release* **99**, 167–176 (2004).
- <sup>63</sup>M. M. Kaneda, S. Caruthers, G. M. Lanza, and S. A. Wickline, *Ann. Biomed. Eng.* **37**, 1922–1933 (2009).
- <sup>64</sup>S.-H. Kim, H. C. Shum, J. W. Kim, J.-C. Cho, and D. A. Weitz, *J. Am. Chem. Soc.* **133**, 15165–15171 (2011).
- <sup>65</sup>J. Wu, T. Kong, K. W. K. Yeung, H. C. Shum, K. M. C. Cheung, L. Wang, and M. K. T. To, *Acta Biomater.* **9**, 7410–7419 (2013).
- <sup>66</sup>H. C. Shum, Y.-J. Zhao, S.-H. Kim, and D. A. Weitz, *Angew. Chem.* **123**, 1686–1689 (2011).
- <sup>67</sup>J. V. M. Weaver, S. P. Rannard, and A. I. Cooper, *Angew. Chem. Int. Ed.* **48**, 2131–2134 (2009).
- <sup>68</sup>I. Pulko, V. Smrekar, A. Podgornik, and P. Krajnc, *J. Chromatogr. A* **1218**, 2396–2401 (2011).
- <sup>69</sup>H. Zhang, G. C. Hardy, Y. Z. Khimyak, M. J. Rosseinsky, and A. I. Cooper, *Chem. Mater.* **16**, 4245–4256 (2004).
- <sup>70</sup>G. Villar, A. D. Graham, and H. Bayley, *Science* **340**, 48–52 (2013).
- <sup>71</sup>A. Imhof and D. J. Pine, *Nature* **389**, 948–951 (1997).
- <sup>72</sup>N. G. Durmus, S. Tasoglu, and U. Demirci, *Nature Mater.* **12**, 478–479 (2013).
- <sup>73</sup>A. C. Hatch, J. S. Fisher, S. L. Pentoney, D. L. Yang, and A. P. Lee, *Lab Chip* **11**, 2509–2517 (2011).
- <sup>74</sup>S. H. S. Lee, M. K. Dawood, W. K. Choi, T. A. Hattton, and S. A. Khan, *Soft Matter* **8**, 3924–3928 (2012).
- <sup>75</sup>C. D. Keating, *Acc. Chem. Res.* **45**, 2114–2124 (2012).
- <sup>76</sup>C. P. Brangwynne, C. R. Eckmann, D. S. Courson, A. Rybarska, C. Hoegel, J. Gharakhani, F. Julicher, and A. A. Hyman, *Science* **324**, 1729–1732 (2009).
- <sup>77</sup>C. A. Ku, J. D. Henry, and J. B. Blair, *Biotechnol. Bioeng.* **33**, 1081–1088 (1989).
- <sup>78</sup>D. N. Cacace and C. D. Keating, *J. Mater. Chem. B* **1**, 1794–1803 (2013).
- <sup>79</sup>Z. Li, S. Y. Mak, A. Sauret, and H. C. Shum, “Syringe-pump-induced fluctuation in all-aqueous microfluidic system – implications for flow rate accuracy,” *Lab Chip* (published online 2013).